

TOWARDS NEARLY ZERO-ENERGY BUILDINGS: THE POTENTIAL OF PHOTOVOLTAIC-INTEGRATED SHADING DEVICES TO ACHIEVE AUTONOMOUS SOLAR ELECTRICITY AND ACCEPTABLE THERMAL COMFORT IN NATURALLY-VENTILATED OFFICE SPACES

Hardi K. Abdullah* and Halil Z. Alibaba

Department of Architecture, Faculty of Architecture, Eastern Mediterranean University, Famagusta, Northern Cyprus, via Mersin 10 Turkey

*Corresponding author: Hardi K. Abdullah, e-mail: hardi.abdullah@su.edu.krd (H.K.A.)

REFERENCE NO	ABSTRACT
ARCH-05	When shading devices are integrated with photovoltaics, the dual-purpose of avoidance of harmful sun exposure and solar electricity generation can be achieved, along with multiple sustainability goals. Researchers have mainly explored the energy demand reduction and electricity production when installing photovoltaic-integrated shading devices (PVISD), while autonomous solar power and indoor thermal comfort aspects have been examined less frequently, particularly in unconditioned buildings. This study investigates the potential of PVISD to satisfy nearly self-sufficient solar electricity and acceptable thermal comfort in a window-based naturally-ventilated office space. Ladybug and Honeybee were employed as the parametric building thermal simulation and analysis tools to perform the required tasks. Microclimate metrics and analysis were utilised to present a spatial map that suggests the traces of passive strategies. The results showed that these passive design means can achieve an adaptive comfort acceptability limit of 80% based on the ASHRAE 55 standard and the PV system generated 70% of the total electricity demand.

Keywords:
Nearly zero-energy buildings (nZEB); autonomous solar electricity; adaptive thermal comfort; passive design strategies; photovoltaic-integrated shading devices (PVISD)

1. INTRODUCTION

The notion of ‘nearly Zero-Energy Buildings’ (nZEB) refers to high energy performance buildings. Introduced by the Energy Performance of Buildings Directive (EPBD) of the European Commission, the policy of nZEB will be implemented from 2020 onwards for all new buildings aiming drastic reductions in greenhouse gas (GHG) emissions. The principle of nZEB requires that the energy demand of a building should be covered to a significant extent by renewable energy resources [1].

Building-Integrated Photovoltaics (BIPV) systems, as the preferable method to harness solar energy [2], are emerging substantially and they are growing in the importance for both academia and the marketplace. One significant aspect of energy efficient buildings is shading devices that can minimise the amount of energy required for cooling and artificial lighting, as well as improve thermal and daylighting qualities [3,4]. As a BIPV technique, photovoltaic-integrated shading devices (PVISD) are thoroughly compatible

with the concept of nZEB and sustainability criteria considering the advantages of reducing quantity of materials and installation spaces needed, as well as lifetime costs. This passive design strategy can have a significant role in obtaining a thermally comfortable space when it is designed effectively. The use of shading devices can offer a cost-effective and aesthetically acceptable means for integrating PV into buildings [5]. External shading systems are under focus for application of photovoltaics especially in the southern orientation [6]. Most related studies focus on energy demand reduction and electricity production while installing PVISD [7], for instance, in the cases of [8] and [9]. On the other hand, the aspect of thermal comfort has been investigated less frequently, particularly in unconditioned buildings.

Achieving nZEB requires the implementation of other passive means such as natural ventilation [10], instead of having a thermally sustainable design by installing more efficient heating, ventilation and air conditioning (HVAC) systems. While eliminating the

assumptions of presupposing HVAC and oversimplified residencies, spatial configuration and passive strategies can have an immense impact on the building's thermal habitability [11]. Thereby, more studies elaborating PVISD are needed to highlight the benefits gained from implementing this practice in terms of enhancing the indoor thermal comfort, daylighting and solar electricity generation in the case of naturally-conditioned spaces.

This paper studies the potential of PVISD to improve the indoor thermal comfort and electricity production in a naturally-conditioned office space in the climate of Famagusta. The study uses only passive design strategies of natural ventilation, solar energy and daylighting control, thus, the role of each technique will be presented and discussed. Occupant-controlled operable windows allow natural ventilation, whereas daylighting control and solar power strategies are employed using the integrated dual-purpose passive technique of PVISD.

2. METHODOLOGY

The study was conducted using a quantitative research approach to computational modelling and simulation techniques to gather and analyse numerical data. Ladybug and Honeybee [12] were employed as the parametric building thermal simulation and analysis tools to perform the required tasks. Ladybug can analyse and visualise data, while Honeybee is used for thermal simulations. This study focuses on the hot Mediterranean weather conditions (dry-summer subtropical climate with moderate seasonality) in Northern Cyprus (i.e., Famagusta) as a climatic scope. An office space was chosen to represent experimental design and specifications for the topic under study. The objective was to investigate the possibility of depending only on passive strategies to satisfy the indoor thermal comfort requirements and self-sufficiency of solar electricity in the case of an unconditioned office room. Thereby, no mechanical cooling or heating systems were installed. Instead, this space was naturally-conditioned only through user-controlled

operable windows. In order to evaluate the impact of PVISD as a passive means, thermal performance simulations were run triple times for all the scenarios: (1) no ventilation and no shading, (2) natural ventilation but no shading (base case thereafter), and (3) natural ventilation with shading (PVISD case thereafter).

2.1. Office space prototype modelling

To demonstrate the impact of PVISD, an office workspace (8.4 m length, 6.0 m width and 3.2 m height) was modelled to dwell 6 person based on the office requirements [13]. This office space comprised a single zone with no internal air walls and two windows located on the south façade. The window-to-wall ratio (WWR) was 30% and the dimensions of a window were 2.52 m × 1.6 m with a sill height of 0.8 m. Assuming that this office room was located on the ground floor of an office building where there were other surrounding spaces beside and above it, the roof and the north-, east-, and west-facing walls were considered adiabatic (Fig. 1).

2.2. Implementing passive design strategies

2.2.1 Construction types and materials

Due to the fact that building materials, as passive means, play a significant role in providing thermal comfort for occupants, this study utilised material properties that are recommended by the ASHRAE 90.1 standard [14] for the climate zone of 3A (encompasses Northern Cyprus). Table 1 demonstrates the construction materials and assembly U-values and R-values, which were assigned to the model design of all specified simulation scenarios.

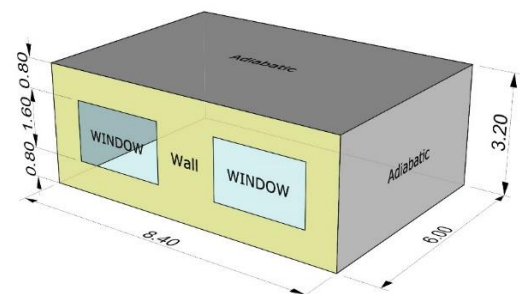


Fig. 1. The modelled office space dimensions and surface conditions.

Table 1. Building construction and assigned materials based on the ASHRAE 90.1–2013 standard.

Construction types	Materials	Thickness (mm)	U_v ($W/m^2\cdot K$)	R_v ($m^2\cdot K/W$)
Floor	Concrete HW	200.0	0.15	6.33
	Floor insulation (R-6 SI)	–		
	Mortar	12.5		
	Porcelain	10.0		
Wall (south-facing)	Stucco	25.0	0.77	1.28
	Concrete HW (or brick)	200.0		
	Mass wall insulation (R-1 SI)	–		
	Gypsum	12.5		
Windows	Clear glass	3.0	2.3	0.42
	Air gap	13.0		
	Clear glass	3.0		

2.2.2 Natural ventilation

Natural ventilation is one of the pioneering strategies of passive design, where occupants use operable windows as a conventional method to arrange indoor space thermal conditions and provide fresh air in naturally-ventilated buildings [15]. Tucci [16] highlighted the potential of natural ventilation in terms of indoor thermal improvement and energy savings in a Mediterranean climate.

In this study, window-based natural ventilation was applied to both the base case and the PVISD case through single side operable windows (no window-driven cross ventilation). As the office space constituted one closed zone and no air walls were assigned, the interior zone air flow rate did not have a significant effect. The fraction of operable glazing area was set to be 50% (sliding windows) and a fraction of operable glazing height was left as the full height of the designed window (1.6 m in this case). Finally, 24 °C was set as the minimum limit of indoor temperature to naturally ventilate the space. To perform the simulation, all the inputs were fed to the Honeybee_Set EP Air Flow component and from there, the Honeybee_Run Energy Simulation was used to assess the thermal performance of the base case and PVISD case scenarios.

2.2.3 Computational design method of PVISD

Nearly in all areas around the studied region, the south façade receives a great amount of solar radiation. Looking at the radiation rose presented in Fig. 2, the annual south radiation in this location reaches 1114.90 kWh/m², which can result in overheating of internal surfaces around an unshaded window. Such an amount can be profitably invested on for electricity production by installing PV modules. Multiple goals are met in implementing the PVISD technique.

Using a parametric climate-based design approach, an external shading device with PV integration was generated. After the simulation of the base case, visualisation of indoor operative temperature revealed that many overheating times occurred in the period between June and November. Therefore, the designated shading element must block sun rays streaming through the windows in this period of time. The Ladybug_AnalysisPeriod component limited the design time span starting from June 10th to November 20th and the hours between 10:00 to 16:00. The specified hours kept the projection of the shading device logical, as the lower sun angles at earlier than 10:00 or later than 16:00 needed a larger shading surface. In spite of restricting the view to the outside, a larger shading depth prevented the useful radiation to warm up the interior space. The Ladybug_SunPath component defined the sun vectors available in this period, then the inputs were used to enable Ladybug_Shading Designer to automatically generate an optimum shading geometry for the studied windows.

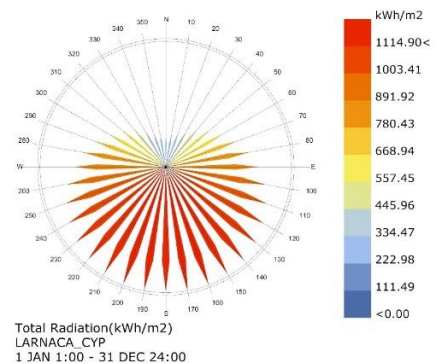


Fig. 2. The radiation rose shows the amount of annual solar radiation received by each orientation.

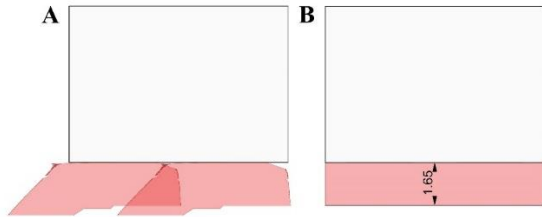


Fig. 3. (A) The automated shading design generation and (B) the refined version.

The automated shading design accounted for each specific sun position to generate the effective device configuration as presented in Fig. 3.A. Restricting the shading length to the exterior boundary of the room (8.4 m), in order to facilitate the PV installation system, the irregular design was refined to have a basic rectangular shape with 1.65 m depth (Fig. 3.B).

This study employed a photovoltaic type called Monocrystalline Silicon for its efficiency and longer life cycle compared to other types. To maximise the efficiency of integrated photovoltaics, a tilt angle is of vital importance. A study assessed the performance of a south-facing fixed PV system with different angles [17]. The results confirmed that tilt angles of 20° to 30° offered the most efficient solutions in terms of producing maximum electricity. Therefore, to acquire the maximal efficiency of the PV and maintain the quality of the shading element (the same horizontal depth of 1.65 m), this study executed a tilt angle of 20° as illustrated in Fig. 4. This decision does not only improve the efficiency of photovoltaics but also increases the PV surface area from 13.86 m² (0°) to 14.75 m² (20°), and thus, more electricity can be produced. The required information—cell efficiency (15%), cost per module (300 U.S. Dollars), power output per module (300 W), inverter efficiency (90%), inverter cost (1000 U.S. Dollars), and replacement time (5 years)—were set as inputs for Honeybee_Generator_PV. Next, the Honeybee_Generation System constituted the system and the output was sent to the Honeybee_Run Energy Simulation using EnergyPlus calculations. The results were visualised through the Honeybee_Visualise Honeybee Generation Cashflow component.

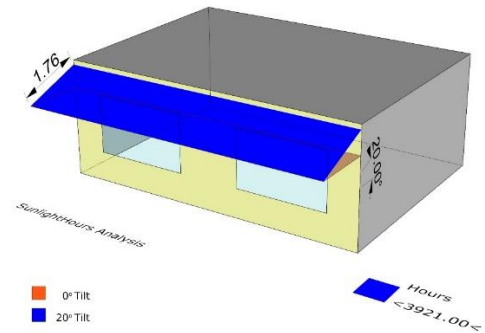


Fig. 4. The 20° tilted photovoltaic-integrated shading device (PVISD) and sunlight hours analysis.

2.3. Thermal performance assessment using adaptive comfort model

This study examined the possibility of using only a passive means to fulfil the standard comfortable criteria. It implemented an adaptive comfort method to quantify the occupants' thermal conditions in terms of being comfortable or not in a given period of time, and thus, evaluating the space based on standard acceptable comfort limits. In order to measure thermal comfort temperature in naturally-ventilated spaces, the ASHRAE 55 standard [18] introduced equation (1)—primarily suits office buildings—based on previous endeavours and studies concerning the adaptive comfort model, such as those by Humphreys and Nicol [19] and Nicol and Roaf [20].

$$T_{\text{comf}} = 0.31 \cdot T_{\text{ref}} + 17.8 \quad (1)$$

where T_{comf} is the indoor comfortable operative temperature (°C) and T_{ref} stands for the prevailing mean outdoor air temperature (°C) for the last 7–30-day time period [21].

The standard defines acceptability limits of 80% ($T_{\text{comf}} \pm 3.5$ °C) for typical applications and 90% ($T_{\text{comf}} \pm 2.5$ °C) when a higher standard of thermal comfort is desired, as shown in Table 2. Thermal performance of the office room was evaluated by total comfortable hours (TCH) followed by percentage of time comfort (PTC), percentage hot (PH), percentage cold (PC), and adaptive comfort (AC) (also called condition of person), where the input conditions were: -1 too cold; 0 comfortable; +1 too hot for occupants—similar to Fanger's [22] PPD and PMV indices, respectively.

Table 2. Acceptability and applicability ranges of adaptive comfort model based on ASHRAE 55–2013 standard.

Acceptability limits	Clothing insulation (clo)	Activity level (met)	Air velocity (m/s)	Operative temperature (°C)	
				Winter	Summer
80%	0.5 – 1.0	1.0 – 1.3	<0.2	23.3	30.3
90%	0.5 – 1.0	1.0 – 1.3	<0.2	24.3	29.3

Ladybug_Adaptive Comfort Calculator was utilised to measure each of the TCH, PTC, PH, PC, and AC values, whereas adaptive comfort chart was generated using the Ladybug_Adaptive Comfort Chart. To understand and analyse the impact of a passive strategy or design decision-making on thermal performance of the office room, three spatial thermal metrics were explored for both the base case (Fig. 1) and the PVISD case (Fig. 4).

2.3.1. Operative temperature (T_o)

It is the primary metric by which adaptive comfort and thermal conditions are measured. The ASHRAE 55 standard [18] defines operative temperature as the weighted average of mean radiant temperature (MRT) and air temperature as expressed in equation (2). Occupants tend to lose half of their body heat through radiation and the other half by air-related factors, such as air temperature and humidity.

$$T_o = A \cdot T_a + (1 - A) \cdot T_{mr} \quad (2)$$

where T_o is the operative temperature (°C), T_a is the indoor air temperature, T_{mr} is the mean radiant temperature, and the coefficient A is a function of the relative air velocity. The operative temperature for moderate thermal environments with the absolute value of the difference between indoor air temperature and mean radiant temperature is ≤ 4 °C, air speed is ≤ 0.2 m/s, thus the value of the constant (A) = 0.5. The equation of the operative temperature can be then expressed as a simple average between T_a and T_{mr} (see equation 3) considering the adaptive model applicability criteria shown in Table 2.

$$T_o = \frac{T_a + T_{mr}}{2} \quad (3)$$

2.3.2. Thermal comfort percent (TCP)

Thermal comfort percent, as a metric to map spatial comfort, is the percentage of time where a given point in space appears inside the adaptive comfort range [23] considering that the conditions constitute being within the desired range. TCP equips designers to communicate the trace of their design decisions in terms of comfort conditions rather than only cooling or heating energy savings [11]. TCP can be interpreted as a loss of comfortable hours and of comfortable space in the analysed period. Occupied thermal comfort percent (occTCP) calculates only the percentage of the occupied hours, which was the intention of this study. Recently, a similar comfort metric was developed and named “Comfort Autonomy (CA)” which is defined as “the percentage of the time occupied over a year where a thermal zone meets or exceeds a given set of thermal comfort acceptability criteria through passive means only” [24]. The office zone under study depended only on passive design strategies; therefore, the results of occTCP resembled CA.

2.3.3. Degrees from target temperature (DTT)

The degrees from target temperature (DTT)—known as adaptive comfort (AC)—metric is the difference in the degree of temperature above or below the ideal indoor operative temperature of adaptive comfort for a specific point in space. This metric enables designers to grasp the reason for a particular design decision being beneficial or harmful and identify the sources that cause discomfort [11]. For example, excessive sun rays penetrating into interior space through a window which result in a point of space being too hot or transcending the adaptive comfort range ($T_{comf} \pm 3.5$ °C for 80% acceptability limit).

3. RESULTS AND DISCUSSIONS

According to the evaluation process explained in the methodology section, this section presents the simulation results and discusses the status of indoor thermal performance of both the baseline and PVISD cases. Information about solar electricity generation and photovoltaic cashflows is articulated.

3.1 Indoor thermal performance of the base case

Using the adaptive comfort model, the thermal performance of the base case office room was evaluated. The results showed that the total comfortable hours (TCH) were 3025 hours out of the 3650 simulated office hours in a year. This number indicates that in 82.87% of the total hours, the office space was comfortable, corresponding 17.13% of time discomfort (PTD). This percentage of time discomfort did not satisfy the criteria of even the 80% acceptability limit of adaptive comfort; nevertheless, the passive strategy of window-based natural ventilation enhanced the thermal performance of this office space by 38.84% or provided 1175 more comfort hours. When the room had only fixed windows or did not provide natural ventilation to cool down the indoor temperature, TCH was 1850 hours or only 50.68% of the time comfortable.

Looking at the operative temperature (Fig. 5), one may realise that the indoor thermal condition of the space remains approximately within the adaptive comfort range of 20.3 °C (lower bound) to 27.3 °C (upper bound)—based on the 80% acceptability limit of the ASHRAE 55 standard [18]—in the greater portion of the office hours except for the summer day times. The T_o reached as high as 33 °C in August and it decreased slightly in the period between June and November. Apparently, the discomfort cold hours happened during the night time, which did not noticeably affect the simulated office hours (08:00–18:00). However, due to assuming adiabatic surfaces (north-, east-, and west-facing walls and the roof) for the simulated model, which eliminates internal heat flows between the possible zones, the night times appeared to be colder than a real situation.

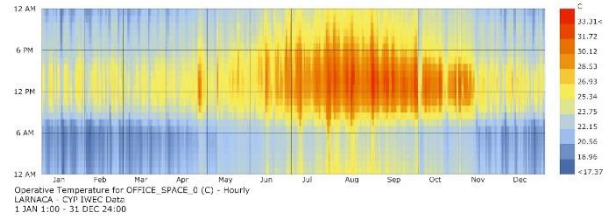


Fig. 5. Annual indoor operative temperature (°C) of the base case office space.

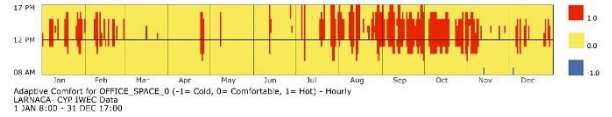


Fig. 6. Adaptive comfort (AC) chart explaining the condition of a person during office hours.

Probably, lower degrees (near the lower temperature bound) at night may be still acceptable by other building programs, such as residential buildings when people spend these times in bed and might not feel too cold. Through visualising the adaptive comfort (AC), the source of discomfort can be understood better. Fig. 6 illustrates the condition of a person feeling hot (red, PH: 17.06%), cold (blue, PC: 0.05%), or comfortable (yellow, PTC: 82.87%). Occupants feel hot in the summer months as a result of drastic sun rays crossing the windows inward. This phenomenon is a major problem that needs to be resolved if obtaining more comfortable hours is desired. Therefore, external shading devices—another profitable passive strategy—are proposed and studied in the following section.

The microclimate map analysis for the selected spatial comfort metrics (T_o , occTCP, and AC) determined the actual sources of discomfort issues. While visualising the microclimate map of the indoor operative temperature (Fig. 7A), the authors noticed that the area near the windows did not meet the adaptive comfort range. At some of these points, the operative temperature was recorded as 33.91 °C, and nearly in one-third of the space, the operative temperature overrode the upper temperature bound of adaptive comfort ($T_o > 27.3$ °C). Moving to the occupied thermal comfort percent visualization (occTCP) (Fig. 7B), it may be observed that there were approximately 12.6 m² space loss and – 625 hours time loss. Fig.

7C shows adaptive comfort (AC) (also called degrees from target temperature (DTT)) describing all the points that remained inside or exceeded the adaptive comfort range ($T_{\text{comf}} \pm 3.5 \text{ }^\circ\text{C}$) based on the 80% acceptability limit. In this case, occupants either feel warm or hardly accept the condition as the indoor operative temperature is noticeably far from the target temperature (0.00 in the figure).

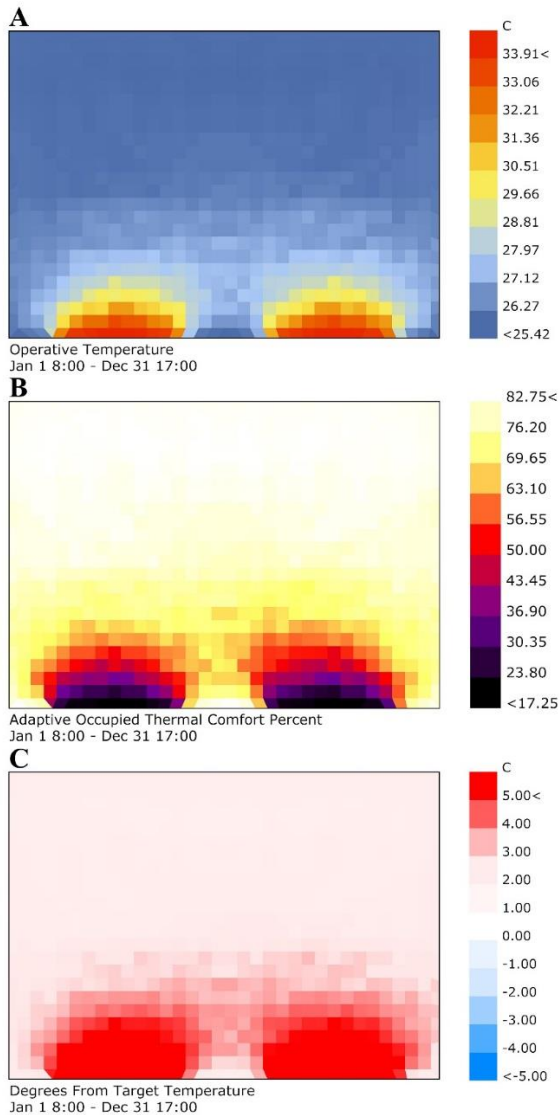


Fig. 7. Base case microclimate map visualisation for the (A) indoor operative temperature (T_o), (B) occupied thermal comfort percent (occTCP), and (C) degrees from target temperature (DTT).

3.2 Indoor thermal performance in the case of PVISD

As an integrated passive strategy, PVISD was supposed to significantly-enhance the indoor thermal quality of the office space,

particularly in the summer period. This intention was achieved when it maximised the total comfortable hours to reach up to 3577 hours. Thereby, 98% of the time, this space was thermally comfortable and only in 2% of the time did it stay uncomfortable (PTD). This shading technique contributed to a reduction in the percentage hot from 17.06% (base case–no shading) to 1.58%. Moreover, the integration of this device boosted thermal comfort percentage by 15.43% compared to the case of no assigned shading by seizing 552 more comfort hours.

In the new adaptive comfort illustration (Fig. 8), it may be noticed that inhabitants feel comfortable during most of the office hours throughout the year. In a few days of July and August, there were afternoon hot degrees which exceeded the upper temperature bound ($27.3 \text{ }^\circ\text{C}$) of the adaptive comfort range. Increasing the air speed is an option to cool down the indoor air temperature and consequently lowering operative temperature. There are numerous ways to raise air seed, but the simplest method might be through using occupant-controlled fans.

The adaptive comfort chart (Fig. 9) demonstrates the boundary of the comfort range for the 80% acceptability limit stated by the ASHRAE 55 [18] standard. This method defines a correlation between indoor operative temperature and prevailing outdoor temperature explaining that residents accept warmer degrees when outdoor air temperature rises. The colourful squares represent the available comfort hours for which the saturated colours in red contain a higher number of desired hours. The black edge polygon indicates the adaptive comfort range. Table 3 clarifies thermal performance of different scenarios and manifests the impact of each integrated passive means on the overall indoor thermal conditions.

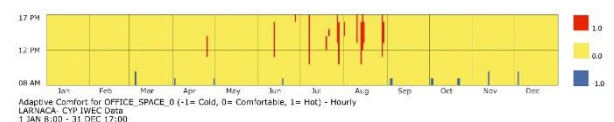


Fig. 8. Adaptive comfort (AC) chart after the integration of passive photovoltaic-integrated shading strategy.

Table 3. The impact of integrated passive strategies on the indoor thermal performance.

Studied criteria	Units	Simulated scenarios		
		Not ventilated/ not shaded	Ventilated/ not shaded	Ventilated/ shaded
Comfort hours (TCH)	hrs	1850	3025	3577
Time comfort (PTC)	%	50.68	82.87	98.0
Percentage hot (PH)	%	49.28	17.06	1.58
Percentage cold (PC)	%	0.02	0.05	0.41
Av. Operative temp. ($T_{o,av}$)	°C	25.25	23.66	22.76
Av. Target temp. ($T_{o,opt,av}$)	°C	23.80	23.80	23.80
Upper temp. bound ($T_{o,up}$)	°C	27.30	27.30	27.30
Lower temp. bound ($T_{o,low}$)	°C	20.30	20.30	20.30
occTCP—time loss	hrs	−1800	−625	−73
occTCP—space loss	m ²	50.4*	12.6	2.4

*All the space area is outside the adaptive comfort range ($T_{comf} \pm 3.5$ °C) of 80% acceptability limit.

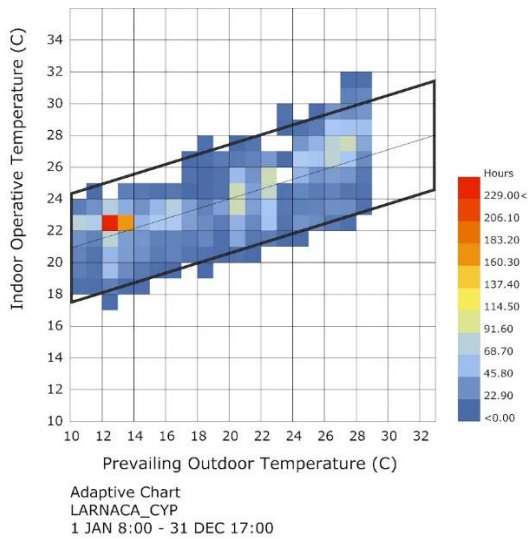


Fig. 9. Adaptive comfort chart of the office space. The black boundary represents comfort range for the 80% acceptability limit based on the ASHRAE 55–2013 standard.

The microclimate map visualisations after the integration of the PVISD system confirmed that there was a significant shift in the indoor thermal quality towards more comfortable space and fulfil the intended acceptability limit. Operative temperature was very close to the ideal degree almost at all points and lowered by 1.5 °C in the overall space temperature. Occupied thermal comfort percent indicated that the space loss decreased to 2.4 m² and total time loss decreased to −73 hours. Adaptive comfort (or degree from target temperature) showed that nearly all the space area recorded the target degree (0.00) or

+ 1 °C, except for a very limited area around the windows (only 2.4 m²).

3.2.1. Photovoltaic system performance

The results of the photovoltaics performance analysis manifested that the 20° tilted system generated 2477.57 kWh/m² annually. This installation angle boosted the production of electricity by 12.83% compared to the 0° installation (2159.60 kWh/m² a year) in this particular location. This enhancement in the output power refers to an increase in solar radiation received by the PV surface that is recorded above 2000.0 kWh/m² annually, as presented in Fig. 10.

As a reason for implementing passive design strategies in the studied office space, the only facility demand was for electrical lighting and equipment, which was predicted as 3574.49 kWh/m² annually by the assigned EnergyPlus-based office program. Therefore, the PV generation system could supply up to 70% of the total electricity demand, while 5526.94 U.S. Dollars will be needed to purchase the rest amount of electricity over the 25 years lifetime of the installed system.

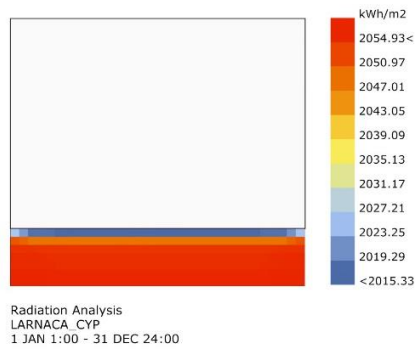


Fig. 10. Solar radiation analysis for 20° tilt Photovoltaic-integrated shading device (PVISD).

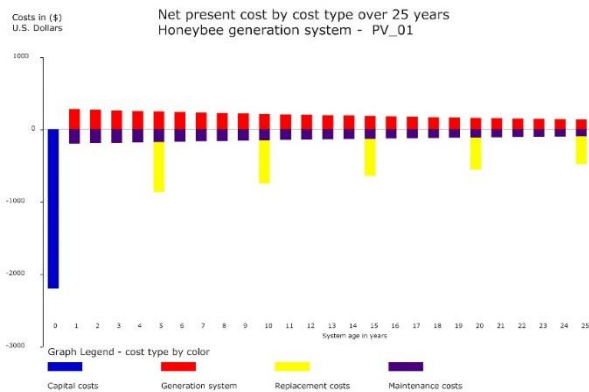


Fig. 11. Photovoltaic (PV) system cash flow over 25 years module lifetime.

More surface area for PV installation (or high-efficiency PV types) is required to achieve zero energy building criteria. Fig. 11 illustrates the generation system cash flow over a 25-year period.

4. CONCLUSION

The most critical building orientation is the south façade and placing a window in the south wall can be challenging. Nevertheless, there is always the opportunity to prevent overheating issues by a novel design of shading devices. In addition to the conventional advantages of this integrated system, contemporary solutions consider green building requirements and recommendations. One option would be replacing the traditional materials of external shading components by PV, which has multiple benefits and assertions to achieve sustainability. As a profitable method towards nZEB, PVISD technique was studied to satisfy the acceptable indoor thermal comfort and nearly self-sufficient solar electricity in a naturally-ventilated office space.

The results indicated that the photovoltaic-integrated shading devices technique, along with other passive strategies such as natural ventilation and construction materials recommended by the ASHRAE 90.1 standard, can achieve an adaptive comfort acceptability limit of 80% based on the ASHRAE 55 standard in the studied office space. As a dual-purpose passive technique, PVISD performed very well in providing 552 more comfort hours (out of 3560 simulated hours) and 10.2 m² more comfort area compared to the base case (only natural ventilation). While implementing PVISD and user-controlled operable windows, 3577 comfort hours (TCH) were recorded, which represents 98% time comfort or less than 2% time discomfort (PTD). By using fans to speed up the air, the small amount of percentage hot (PH) felt by occupants in the summer months can be eliminated. The PV system of the shading device generated 70% of the total electricity demand for the office electrical lighting and equipment by generating 2477.57 kWh/m² annually. The office room needs more surface area for PV installation (or high-efficient PV types) if reaching autonomous solar electricity is desired.

As an ongoing research, the next endeavour encompasses daylighting evaluation and using multi-objective optimisation techniques to find trade-offs among various optimisation objectives and intended performance criteria.

References

- [1] Boermans, T.; Hermelink, A.; Schimschar, S. Principles for Nearly Zero-Energy Buildings—Paving the way for effective implementation of policy requirements. Ecofys, Danish Building Research Institute (SBI), Building Performance Institute Europe (BPIE), Brussels, Belgium, November 2011.
- [2] Peng, C.; Huang, Y.; Wu, Z. (2011), Building-integrated photovoltaics (BIPV) in architectural design in China, *Energy and Buildings*, vol. 43, 12, 2011, pp. 3592–3598.
- [3] Miran, F. D.; Abdullah, H. K. Evaluation of the Optimal Solar Shading Devices for Enhancing Daylight Performance

of School Building (A case study of semi-arid climate—Erbil city). *ZANCO Journal of Pure and Applied Sciences*, 28, 2, 2016, pp. s580–598.

[4] Al- Tamimi, N. A.; Fadzil, S. F. S. The potential of shading devices for temperature reduction in high-rise residential buildings in the tropics. *Procedia Engineering*, 21, 2011, pp. 273–282.

[5] Palmero-Marrero, A. I.; Oliveira, A. C. Evaluation of a solar thermal system using building louvre shading devices. *Solar energy*, 80, 5, 2006, pp. 545–554.

[6] Dubois, M. C. A simple chart to design shading devices considering the window solar angle dependent properties. In Proceedings of the EuroSun 2000: ISES-Europe Solar Congress, Copenhagen, Denmark, 2000, 3, pp. 18–22.

[7] Ibraheem, Y.; Farr, E. R.; Piroozfar, P. A. Embedding passive intelligence into building envelopes: a review of the state-of-the-art in integrated photovoltaic shading devices. *Energy Procedia*, 111, 2017, pp. 964–973.

[8] Abdullah, H. K.; Alibaba, H. Z. Retrofits for Energy Efficient Office Buildings: Integration of Optimized Photovoltaics in the Form of Responsive Shading Devices. *Sustainability*, 9, 2017, pp. 2096.

[9] Mandalaki, M.; Konstantinos, Z.; Theocharis, T.; Alexandros, V. Assessment of fixed shading devices with integrated PV for efficient energy use. *Solar Energy*, 86, 2012, pp. 2561–2575.

[10] Allard, F.; Santamouris, M. *Natural ventilation in buildings—A design handbook*. London: Earthscan Publication Ltd., 1998.

[11] Mackey, C. W. Pan climatic humans: shaping thermal habits in an unconditioned society. Master thesis, Massachusetts Institute of Technology, 2015.

[12] Roudsari, M. S.; Pak, M. Ladybug: a parametric environmental plugin for Grasshopper to help designers create an environmentally-conscious design. In Proceedings of the BS2013: 13th conference of International Building Performance

Simulation Association, Chambéry, France, 2013, 13, pp. 3128–3135.

[13] Voss, J. *Revisiting office space Standards*. Grand Rapids, MI: Haworth, Inc, 2000.

[14] ASHRAE Standard 90.1—Energy Standard for Buildings Except Low-Rise Residential Buildings, Atlanta, GA: American Society of Heating, Refrigerating, and Air-Conditioning Engineers, 2013.

[15] Brager, G. S.; de Dear, R. Climate, comfort, & natural ventilation: a new adaptive comfort standard for ASHRAE standard 55. In Proceedings of the International Conference Moving Thermal Comfort Standards into the 21st Century, Oxford Brookes University, Windsor, UK, 2, 2001, pp. 1–18.

[16] Tucci F. Passive Cooling in Mediterranean Area for a Bioclimatic and Zero Energy Architecture. In: Sayigh A. (eds) *Mediterranean Green Buildings & Renewable Energy*, Springer, Cham, 2017, pp. 773–783.

[17] Hwang, T.; Kang, S.; Kim, J. T. Optimization of the building integrated photovoltaic system in office buildings—Focus on the orientation, inclined angle and installed area. *Energy and Buildings*, 46, 2012, pp. 92–104.

[18] ASHRAE Standard 55—Thermal environmental conditions for human occupancy, Atlanta, GA: American Society of Heating, Refrigerating and Air-Conditioning Engineers, 2013.

[19] Humphreys M. A; Nicol J. F. Understanding the adaptive approach to thermal comfort, field studies of thermal comfort and adaptation. *ASHRAE Technical Data Bulletin*, 14, 1, 1998, pp.1–14.

[20] Nicol, F.; Roaf, S. Pioneering new indoor temperature standards: the Pakistan project. *Energy and Buildings*, 23, 3, 1996, pp. 169–174.

[21] deDear R. J.; Brager G. S. Thermal comfort in naturally ventilated buildings: revisions to ASHRAE Standard 55. *Energy and Buildings*, 34, 6, 2002, pp.549–61.

[22] Fanger, P. O. *Thermal comfort: Analysis and applications in environmental engineering*. New York: McGraw-Hill, 1970.

[23] Rakha, T. Towards comfortable and walkable cities: spatially resolved outdoor thermal comfort analysis linked to travel survey-based human activity schedules. Doctoral thesis, Massachusetts Institute of Technology, 2015.

[24] Levitt, B.; Ubbelohde, M.; Loisos, G.; Brown, N. Thermal autonomy as metric and design process. In Proceedings of Pushing the Boundaries: Net positive Buildings (SB13), Vancouver, Canada, 5, 2013, pp. 47–58.